The ESR Spectrum of a π Cation Radical Trapped in a Single Crystal of Chloro(tetraphenylporphyrinato)cobalt(III)

Masahiro KOHNO,* Hiroaki OHYA-NISHIGUCHI,† Kiyoko YAMAMOTO,†† and Tosio SAKURAI††

JEOL Ltd., Akishima, Tokyo 196

† *Department of Chemistry, Faculty of Science, Kyoto University, Sakyo-ku, Kyoto 606*

†† *The Institute of Physical and Chemical Research, Wako, Saitama 351*

(Received March 20, 1982)

The electron-spin-resonance (ESR) spectra of three paramagnetic species trapped in single crystals of chloro(tetraphenylporphyrinato)cobalt(III) have been observed at 77 K. Using the ESR parameters obtained, one of them has been identified as the $[Co^{III}(tpp)]^{2+}\cdot(Cl^-)_2$ π cation radical, and the other two species, as $[Co^{II}(tpp)]$ which are influenced by axial ligation. From the angular variations in the hfcc due to the ^{59}Co, ^{14}N, and ^{35}Cl in the π cation radical, it has been found that the unpaired electron resides on the a_{2u} porphyrin π orbital and polarizes the Co and Cl atomic orbitals through a spin-polarization mechanism. Finally, the radical formation mechanisms in solution are briefly discussed, based on the results obtained from the single-crystalline measurements.

The role of the porphyrin-cation radicals in the chemical and biological behavior of metalloporphyrins has become very important. In the enzymatic reaction of horse-radish peroxidase (HRP) with peroxide, for example, it has been pointed out that the HRP I has an electronic configuration of Fe(IV) ($S=1$), with the porphyrin ring forming an a_{2u} π cation radical.[1] On the other hand, Dolphin *et al.*[2] showed how the organic macrocycles play important roles in biochemical systems in addition to those of the centrally coordinated metals.

It has been previously shown by ^1H FT-NMR[3] and ESR studies[4] that diamagnetic chloro(tetraphenylporphyrinato)cobalt(III) (**A**) (Fig. 1) in chlorinated solvents changes partially into paramagnetic species upon thermal and light activations. The formation of this species in the solutions occurs reversibly, with small enthalpy differences. This species was identified as a π cation radical of cobalt(III) tetraphenylporphyrin, $[Co^{III}(tpp)]^{2+}\cdot(Cl^-)_2$, using an electrochemical ESR technique[5]. The formation of the cation radical under ambient conditions can, therefore, be closely related to the enzymatic reactions of the metalloporphyrins mentioned above.

In the course of a crystallographic investigation of **A**[6] it was expected that the crystals grown from a solution including such paramagnetic species may trap the species. It may, therefore, be appropriate to elucidate in detail the electronic structure and the mechanism of its formation in solutions by using the single crystals trapping the species. In agreement with this expectation, we have succeeded in observing the ESR spectra of paramagnetic species trapped in the single crystals, one of which has been identified as the π cation radical. In order to clarify further the electronic structure of the radical, we have carried out a detailed ESR investigation of the single crystals.

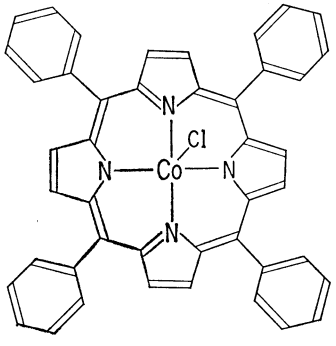

Fig. 1. Chloro($\alpha,\beta,\gamma,\delta$-tetraphenylporphyrinato)cobalt(III).

In this paper we will first describe the ESR parameters obtained from the angular dependences of the ESR spectra due to the paramagnetic species in the single crystals of **A**. Second, the electronic structure of the cation radical will be discussed in detail based on the parameters thus obtained and those in solutions reported previously. Finally, the mechanisms of its formation in solutions will be presented in relation to that of HRP I.

Experimental

A was prepared by using a method previously reported.[6] The compound obtained from the methanol solution was dissolved in chloroform or dichloromethane, and the solvent was allowed to evaporate slowly to yield violet and lustrous crystals of **A**. The purity of the crystals obtained was examined by means of elemental analysis and visible-spectrum measurements (Found: C, 73.40; H, 4.20; N, 7.84; Co, 8.24; Cl, 5.06%. λ_{max} (ε) in CH_2Cl_2: 544 nm(13200) and 406 nm(112000)). The spontaneous evaporation of the solvent gave crystals of various external forms; obelisk, pyramid, and bulky shapes. Previously the results of a X-ray analysis of the obelisk crystals were reported.[6] The successive refinement of the structure analysis[7] of these crystals made clear the existence of oxygen at the 6th ligand position.

Their crystal parameters, as determined by the X-ray diffraction method, are listed in Table 1. The pyramid and obelisk crystals were submitted to the ESR measurements. In the case of the obelisk crystal, the c axis was perpendicular to the porphyrin plane and parallel to the Co–Cl bond, which corresponds to the molecular symmetry axis and coincides with the long crystal axis. The basal plane of the pyramid crystal coincides with the molecular plane and is perpendicular to the c axis. The relationships between the a and b axes and the external forms are illustrated in Fig. 2. The angle between the a axis and one of the molecular symmetry axes parallel to the Co–N bond was 15°.[6] Such crystal habits were utilized for the single-crystal

Table 1. Crystal parameters of $Co^{III}(tpp)Cl$

Form	System	Lattice constants a/Å	c/Å	U/Å^3	Space group	Z	D_o	D_c
Obelisk	Tetragonal	13.693(2)	9.701(2)	1818.9(6)	14	2	1.34_7	1.324
Pyramid	Tetragonal	13.450(5)	9.792(3)	1771.4(11)	14	2	1.35_6	1.359

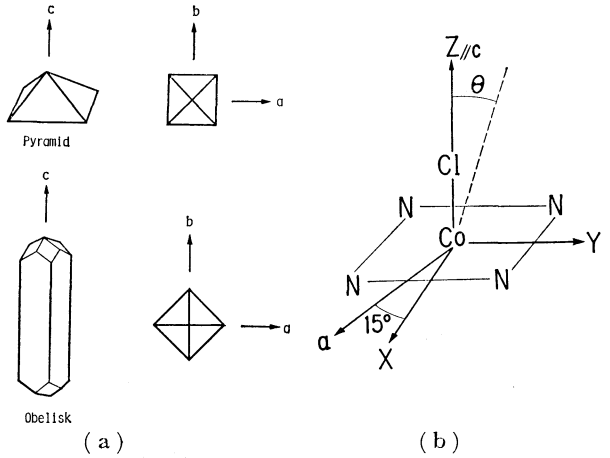

Fig. 2. (a) Crystal axis in pyramid and obelisk type crystals of A. (b) Relationship between crystal axis and molecular axis.

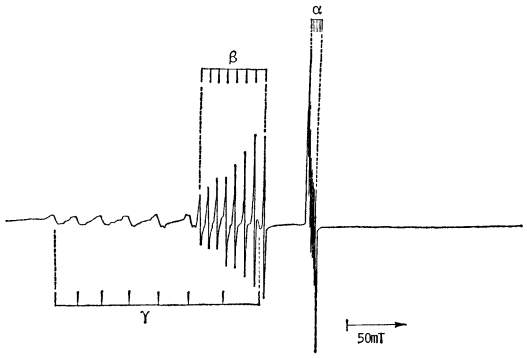

Fig. 3. The ESR spectrum of paramagnetic species trapped in a pyramid type single crystal of **A** at 77 K ($H_0 \perp c$).
Note that three paramagnetic species, α, β, and γ are clearly distinguished.

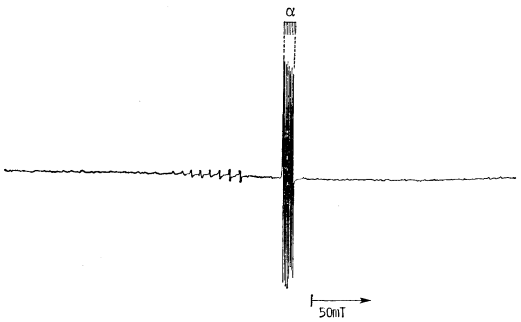

Fig. 4. The ESR spectrum of paramagnetic species trapped in an obelisk type single crystal of A at 77 K ($H_0 \perp c$).
Note that the gain of the ESR observation is about 10 times larger than that of Fig. 3.

ESR measurements. Typical sizes of the obelisk and pyramid crystals used for the measurements were $0.1 \times 0.1 \times 0.3$ cm^3 and $0.2 \times 0.2 \times 0.1$ cm^3 respectively.

The ESR spectra were recorded on a JEOL X-band FE-3X ESR spectrometer. The spin concentrations of the paramagnetic species were determined from a comparison of the intensity of the signals with that of 2,2,6,6-tetramethyl-4-hydroxyl-1-piperidyl oxyl (98%) used as a standard. In order to obtain the ESR parameters of the paramagnetic species, the resonance magnetic field and the microwave frequency of each absorption line were measured using a JEOL ES-FC-4 NMR gaussmeter and a Takeda Riken TR5211 frequency counter respectively. The ESR parameters were determined by the best fitting of the experimental data with an equation derived by the second-order perturbation theory.[8] The computer simulation for the hyperfine structure analysis was carried out using a JEOL ES-9835 computer system.

Results and Discussion

*The ESR Spectra of the Paramagnetic Species in the Single Crystal of **A**.* It has already been determined from the magnetic susceptibility measurements that **A** is diamagnetic in the range from 77 K to room temperature.[6] Therefore, the ESR signals obtained from the crystals are regarded as those due to paramagnetic species trapped in the diamagnetic matrix. Figure 3 shows the ESR spectrum of the paramagnetic species in a pyramid crystal of **A** with the crystal setting of $H_0 \perp c$ at 77 K. The spectrum is composed of three signals, each of which has the hyperfine (hf) structure characteristic of ^{59}Co with $I=7/2$. Their microwave power and the temperature dependences of the signal intensities were different from one another. Therefore the spectrum was regarded as a superposition of the hf patterns due to three different species. Hereafter, we will call them α, β, and γ species, from right to left in the spectrum shown in Fig. 3. The relative intensities of these signals, that is, the relative amounts of these species, depended on the conditions of the crystallization and the external forms. The signal intensities due to these species in the pyramid crystal were of comparable orders of magnitude. On the other hand, the spectrum obtained from the obelisk crystal showed mainly the hf pattern due to the α species, as is shown in Fig. 4.

The angular variations in the absorption lines due to these species were measured on a plane including the c axis and on the ab plane which corresponds to the molecular plane of porphyrin. Table 2 lists the observed parameters of ^{59}Co in these species. The parameters obtained from the pyramid and obelisk crystals coincided with each other within the range of experimental errors. The g values of the β and γ

species are very similar to those of Co^{II}(tpp) in H_2-(tpp),[9] they are also listed in Table 2. The results are good enough to conclude that the β and γ species correspond to Co^{II}(tpp) in H_2(tpp), although the hfcc are a little different. The small deviations from the data reported earlier[9] may be due to slightly different perturbations from the axial ligands. The electronic configurations of Co^{2+} are very sensitive to axial ligands, as has already been pointed out.[10] The details of the discussion of the electronic structures of these species will be published elsewhere. The existence of the Co^{II} species in the crystals means their formation in solution, which provides an important clue to the mechanism of the formation of the π cation radical in solution, as will be described in the last section.

π Cation Radical of Cobalt(III) Tetraphenylporphyrin. The angular dependences of the ESR spectra of the α species were observed in the obelisk and pyramid crystals. The hf structure due to the α species in the pyramid crystal overlapped with those due to the β and γ species. Fortunately, the obelisk crystal showed mainly the signals due to the α species. Therefore, the angular dependence of the spectrum was measured by using the obelisk crystal.

The angular-dependent spectra of the α species on the ab plane and on the plane including the c axis are shown in Fig. 5. The spectra about the c axis (Fig. 5a) are angular-independent and have only eight hf lines due to ^{59}Co with an appreciably broad line width, the g value and the hfcc of ^{59}Co being 1.9980± 0.0001 and 1.25 mT respectively. On the other hand, in Fig. 5b, the eight hf lines for $H_0 \perp c$ gradually coalesce into one broad distorted line, as the angle between the direction of the magnetic field and the c axis, (θ), increases. The coalesced line at about θ= 40—50° splits into many lines at the higher angles. The small, sharp line at the center is due to an impurity in the crystal. It should be noted here that the g value is constant within the range of experimental errors (±0.0001) in this experiment. The spectrum for $H_0//c$ consists of 28 lines with a line-width (ΔH) of about 0.3 mT and with g=1.9981±0.0001. The spectrum simulation was carried out using one cobalt $a_{^{59}Co}$= 1.13 mT, four nitrogens $a_{^{14}N}$=0.56 mT, two chlorines $a_{^{35}Cl}$=0.57 mT ($a_{^{37}Cl}$=0.50 mT), and ΔH=0.40 mT,

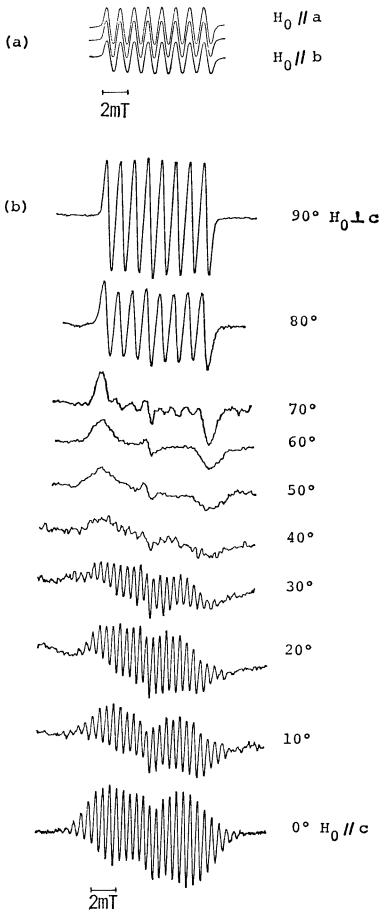

Fig. 5. The angular dependent ESR spectra of α species, (a): rotation about c axis, (b): rotation from the c axis to an axis perpendicular to the c axis.

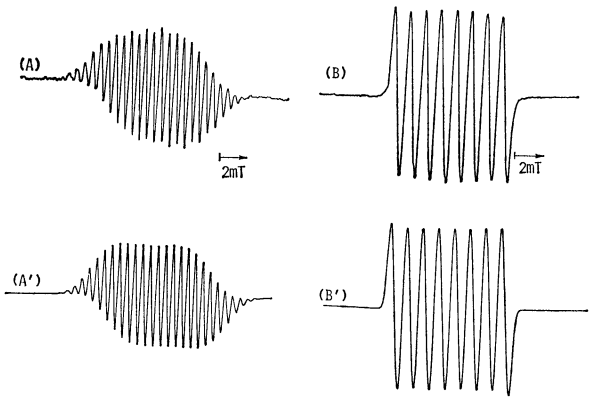

Fig. 6. The ESR spectra of the α species trapped in a single crystal of A at 77 K, (A) at $H_0//c$ and (B) at $H_0 \perp c$.
Simulation (A') assumes one cobalt a_{Co}=1.13 mT, four nitrogens a_N=0.56 mT, and two chlorines $a_{^{35}Cl}$= 0.57 ($a_{^{37}Cl}$=0.50) mT and (B') assumes one cobalt a_{Co}=1.18 mT.

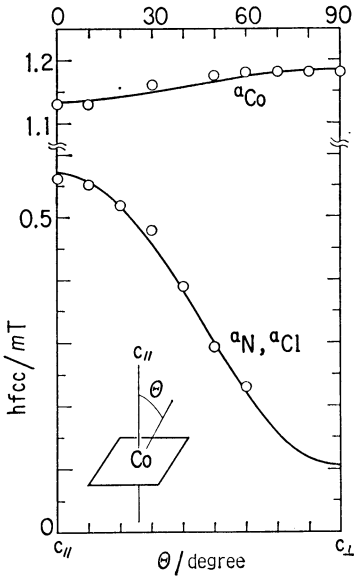

Fig. 7. The angular dependent hfcc of cobalt, nitrogen, and chlorine atoms.
○: Observed value, ——: calculated value.

TABLE 2. ESR PARAMETERS OF PARAMAGNETIC SPECIES TRAPPED IN THE SINGLE CRYSTALS OF **A**

Species	$g_\perp$	$g_{//}$	A_{Co} 10^{-4} cm^{-1}		A_N 10^{-4} cm^{-1}		A_{Cl} 10^{-4} cm^{-1}		
			$A_\perp$	$A_\parallel$ c)	$A_\perp$	$A_\parallel$ c)	$A_\perp$	$A_\parallel$ c)	
α, $[Co^{III}(tpp)]^{2+}(Cl^-)_2$	1.9980 (±0.0001)	1.9981 (±0.0001)	12 (±0.1)	10 (±0.1)	0.9 (±0.1)	5.2 (±0.1)	1.0 (±0.1)	5.2 (±0.1)	a)
β	2.5273 (±0.0003)	1.9964 (±0.0003)	97 (±3)	105 (±3)					a)
γ	3.241 (±0.001)	1.745 (±0.001)	401 (±3)	192 (±3)					a)
Co^{II}(tpp) in H_2(tpp)	2.505	2.034	92	115					b)
Co^{II}(tpp) in H_2(tpp)	3.322	1.798	395	197					b)

a) This work. b) Ref. 9. c) The parallel direction of A values of Co, N, and Cl coincides with the z axis of the molecule.

which led to the best fit to the experimental data. The simulation spectra are shown in Fig. 6. The simulation at various angles was successively carried out by changing the parameters mentioned above, shown in Fig. 7, as functions of θ. The hfcc values of ^{14}N and $^{35}Cl(^{37}Cl)$ have a maximum at $\theta=0°$ ($H_0//c$) and a minimum at $\theta=90°$ ($H_0\perp c$), but that of ^{59}Co is almost independent of θ; its small anisotropic part has a maximum at $\theta=90°$ ($H_0\perp c$). The principal values of g and hfcc are also summarized in Table 2.

The g value obtained was isotropic and very close to that of the free electron (2.0023). The difference in these values is probably due to contributions from unoccupied orbitals of the cobalt atom. The isotropic parts of the ^{59}Co, ^{14}N, and $^{35}Cl(^{37}Cl)$ were also very close to those of the π cation radical of Co^{III}(tpp) obtained by the electrochemical oxidation of Co^{II}(tpp) of **A**.[5] Therefore, one can, from these data, identify the α species as the π cation radical of Co^{III}(tpp) coordinated by two chlorines.

Electronic Structure of the π Cation Radical of $[Co^{III}(tpp)]^{2+\cdot}$. It was well established that the neutral species Co^{II}(tpp) is paramagnetic, with an effective electron spin of 1/2 and with a square-planar $3d^7$ configuration, $(3d_\pi)^4$ $(3d_{xy})^2$ $(3d_{z^2})$. In the present case, the β and γ species showed the ESR parameters characteristic of this configuration. On the other hand, as we reported previously,[5] the π cation radical of $[Co^{III}(tpp)]^{2+\cdot}$, generated by electrochemical oxidations of Co^{II}(tpp) or **A** in solutions, has an electronic configuration described by a combination of diamagnetic Co^{3+} and paramagnetic tpp ligands, $(3d_\pi)^4$ $(3d_{xy})^2$ $(a_{2u})^1$. The a_{2u} π orbital has a spin distribution characterized by an appreciable localization (76%) at meso-carbons, followed by a 20% spin density at four nitrogens. This spin distribution of the π cation radical was experimentally confirmed by the observation of the angular dependent hfcc values of cobalt and four nitrogen atoms, $a_{Co}(\theta)$ and $a_N(\theta)$, in the single crystal, as is shown in Fig. 7.

The $a(\theta)$ is expressed by a combination of the isotropic (A_{iso}) and the anisotropic (A_{aniso}) parts of the hfcc:

$$a(\theta) = A_{aniso}(3\cos^2\theta - 1) + A_{iso} \quad (1)$$

$$A_{iso} = (A_\parallel + 2A_\perp)/3 \quad (2)$$

where $A_\parallel$ and $A_\perp$ are the values of $a(\theta)$ at $\theta=0°$ and 90° respectively. The best fit of the equations to the experimental values, as is shown in Fig. 7, has lead to the values of $A^N_{iso}=0.26$ mT and $A^N_{aniso}=0.15$ mT. A^N_{iso} is very close to that of $[Co^{III}(tpp)]^{2+\cdot}(Cl^-)_2$ in solution (0.28 mT). This confirms the appropriateness of the identification of the α species as the π cation radical. From $A^N_{iso}=0.26$ mT, the spin density at the 2s orbital of nitrogen is calculated as $0.26/55.7=0.0047$ by using a theoretically estimated hfcc.[11] The anisotropic part in Eq. 1 provides also useful information about the contribution of the nitrogen orbitals to the a_{2u} orbital. First, $a_N(\theta)$ has a maximum at $\theta=0°$. This means that the axis of the $2p_z$ orbital of the nitrogen coincides with the c axis of the crystal. Second, the A^N_{aniso} is another measure of the spin density on the nitrogen $2p_z$ orbital. When we use the hfcc of the nitrogen $2p_z$ orbital of 1.7 mT[11] the spin density of one of the four nitrogen atoms ($\rho^N_{2p_z}$) is estimated as 0.088. This value coincides with that obtained from the spectra in solution (5 to 10%).

The chlorine hfcc showed the same angular dependence as the nitrogens; thus $A^{Cl}_{iso}=0.26$ mT and $A^{Cl}_{aniso}=0.15$ mT. A similar estimation of the spin density on the chlorine atom has lead to the values of $\rho^{Cl}_{3s}=0.0016$ and $\rho^{Cl}_{3p_z}=0.029$.[11] It should be noted here that the spin polarization in the $3p_z$ orbital is dominant. Although numerous ESR studies have revealed interactions of diamagnetic cations with aromatic anion radicals,[12] it was not until recently that the opposite interaction of diamagnetic anions with cation radicals[13] was detected. In order to clarify the mechanism of the interaction, it is instructive to compare the A^{Cl}_{iso} and A^N_{iso} in our system with those in some analogous systems, $[M^{II}(tpp)]^{+\cdot}Cl^-$: 0.152 and 0.151 mT for M=Mg, 0.162 and 0.166 mT for M=Zn, and 0.185 and 0.182 mT for M=Cd,[13] respectively. These data show clearly that A^{Cl}_{iso} depends linearly on A^N_{iso}, as in the case of A^{Co}_{iso} with A^N_{iso} reported previously. Therefore, it is concluded that the chlorine hfcc results from the spin polarization by the π electron on the nitrogen atoms.

The unpaired π electron on the nitrogen $2p_z$ orbital polarizes the four nonbonding orbitals of the nitrogens. A combination of these orbitals with total symmetry mixes well with the $3d_{z^2}$ and 4s orbitals of the cobalt atom. The ^{59}Co hfcc ($A^{Co}_{Iso}=1.16$ and $A^{Co}_{anIso}=-0.03$ mT) showed a small angular dependence, different from those due to ^{14}N and ^{35}Cl. The estimated spin densities, ρ^{Co}_{4s} and $\rho^{Co}_{3d_{x^2-y^2}}$ at the cobalt nucleus were $1.16/130.8=0.009$ and $-0.03/7.65=-0.04$ respectively, which were estimated based on the values of the hfcc calculated for the Co^0 configuration of $3d^74s^2$.[11] The spin density at the cobalt nucleus is of the same order of magnitude as those at the two chlorine nuclei. This means that the polarizations at these nuclei are a result of the first-order in the perturbation induced by the unpaired electron which resides on the nitrogen π orbital. Therefore, the other possibility that the electrons at the two chlorine nuclei are polarized through the cobalt atom, of the second-order in the effect, can be neglected. Figure 8 shows a schematical drawing of the spin polarization mentioned above with capable atomic orbitals. In summary, the unpaired π electron on four nitrogen atoms polarizes the electrons on two chlorine nuclei and the cobalt nucleus through the spin-polarization mechanism, the orders of the polarization being about 0.03 and 0.01 respectively.

On the Mechanism of the Cation Radical Formation. As described in the previous papers,[3,4] the π cation radical is formed by thermal activation in the chlorinated solvents. The formation of the species occurs reversibly with small enthalpy differences (ΔH). From the exponential portion of the temperature dependences of the spin concentration, ΔH was estimated to be 4 kJ mol^{-1} in tetrachloroethane and 10 kJ mol^{-1} in dichloromethane.[4] These results may indicate phenomenologically an equilibrium between the paramagnetic species (α, β, and γ) and the diamagnetic species, (**A**):

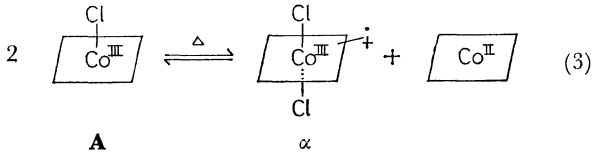

(3)

From the ESR measurements described above, it has been found that the crystals grown from the chlorinated solvents trap Co^{II}(tpp) (β and γ) in addition to the π cation radical (α). This fact apparently supports the hypothesis of Eq. 3. However, the detailed examination of Eq. 3 provides several possibilities as to the elementary reactions. The existence of oxygen in the atmosphere and the natural-light irradiation over the procedure of the sample preparations also induce the radical formation.

In conclusion, it should be understood that the observation of three paramagnetic species in our systems supports the apparent equilibrium of Eq. 3 described as a result of several reactions undetectable by the ESR techniques.

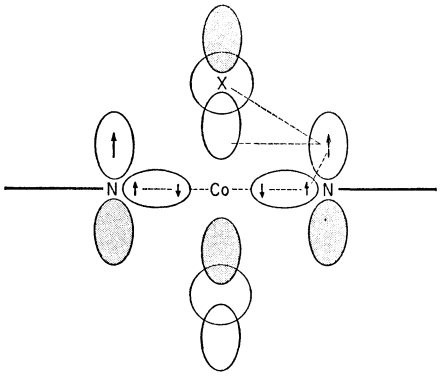

Fig. 8. Schematical drawing about the spin polarization on the cobalt, nitrogen, and halogen atoms in $[Co^{III}(tpp)]^{2+}\cdot(X^-)_2$.

References

1) G. H. Loew and Z. S. Herman, *J. Am. Chem. Soc.*, **102**, 6173 (1980), and the other references cited therein.
2) D. Dolphin, A. W. Addison, M. Cairns, R. K. Dinello, N. P. Farrell, B. R. James, D. R. Paulson, and C. Welborn, *Int. J. Quant. Chem.*, **16**, 311 (1979).
3) K. Yamamoto, J. Uzawa, and T. Chijimatsu, *Chem. Lett.*, **1979**, 89.
4) K. Yamamoto, M. Kohno, and H. Ohya-Nishiguchi, *Chem. Lett.*, **1981**, 255.
5) H. Ohya-Nishiguchi, M. Kohno, and K. Yamamoto, *Bull. Chem. Soc. Jpn.*, **54**, 1923 (1981).
6) T. Sakurai, K. Yamamoto, H. Naito, and N. Nakamoto, *Bull. Chem. Soc. Jpn.*, **49**, 3042 (1976).
7) T. Sakurai and K. Yamamoto, Proceedings of the 30th Annual Meeting of Coordination Chemistry (1980), p. 106.
8) G. Bleaney, *Philos. Mag.*, **42**, 441 (1951).
9) J. M. Assour, *J. Chem. Phys.*, **43**, 2477 (1965).
10) W. C. Lin, "Electron Spin Resonance and Electronic Structure of Metalloporphyrins," in "The Porphyrins," ed by D. Dolphin, Academic Press, New York and London (1979), Vol. 4, p. 355.
11) K. Kuwata and K. Ito, "Denshi-spin-kyomei Nyumon," Nankodo, Tokyo (1980), Chap. 2.
12) For example, F. Gerson, "High Resolution ESR Spectroscopy," John Wiley & Sons and Verlag Chemie (1970), p. 137.
13) J. Fajer and M. S. Davis, "Electron Spin Resonance of Porphyrin π Cations and Anions," in "The Porphyrins," ed by D. Dolphin, Academic Press, New York and London (1979), Vol. 4, p. 198, and the other references cited therein.